International Journal of Chronic Obstructive Pulmonary Disease Dovepress
open access to scientific and medical research

Open Access Full Text Article

ORIGINAL RESEARCH

Effective-Component Compatibility of Bufei Yishen Formula III Suppresses Mitochondrial Oxidative Damage in COPD: Via Pkm2/Nrf2 Pathway

Yang Liu[1], Lanxi Zhang[2], Jie Zhao[1,3], Ruilong Lu[1], Xuejie Shao[1], Kexin Xu[1], Jiansheng Li[1,3,4,*], Yange Tian[1,3,*]

[1]Collaborative Innovation Center for Chinese Medicine and Respiratory Diseases Co-Constructed by Henan Province and Education Ministry of People's Republic of China, Henan University of Chinese Medicine, Zhengzhou, People's Republic of China; [2]School of Basic Medicine (Zhongjing School), Henan University of Chinese Medicine, Zhengzhou, People's Republic of China; [3]Henan Key Laboratory of Chinese Medicine for Respiratory Disease, Henan University of Chinese Medicine, Zhengzhou, People's Republic of China; [4]First Affiliated Hospital of Henan University of Chinese Medicine, Zhengzhou, 450000, People's Republic of China

*These authors contributed equally to this work

Correspondence: Jiansheng Li; Yange Tian, Email li_js8@163.com; yange0910@126.com

Purpose: The main objective of this study was to explore the mechanism of effective component compatibility of Bufei Yishen formula III (ECC-BYF III) in inhibiting mitochondrial oxidative stress in a rat model of chronic obstructive pulmonary disease (COPD).

Methods: A549 cells exposed to cigarette smoke extract (CSE) were used to establish a model of mitochondrial oxidative damage. The cells were treated with the plasmid encoding Pkm2 and the enzymes and proteins involved in oxidative stress and mitochondrial function were measured. A rat model of COPD was established using CS and bacteria. Two different treatments were established, ECC-BYF III (5.5 mg/kg/d) and N-acetylcysteine (54 mg/kg/day). Animals were tested for pulmonary function (Vt, PEF, FVC, FEV0.1s and Cdyn) after eight weeks of therapy and were sacrificed. Pulmonary H&E staining was performed, and the total superoxide dismutase (T-SOD), glutathione peroxidase (GSH-Px), total antioxidant capacity (T-AOC), and malondialdehyde (MDA) content were measured. The mitochondrial function was also examined. Furthermore, the Pkm2/Nrf2 signaling pathway was evaluated.

Results: Overexpression of Pkm2 dramatically ameliorated the CS-induced mitochondrial oxidative damage. Further studies indicated that ECC-BYF III significantly improved mitochondrial function and inhibited oxidative stress in the lung tissues of COPD rats. Moreover, it can upregulate mitochondrial respiratory chain enzyme activity. ECC-BYF III also decreased the MDA content and increased T-SOD, GSH-Px, and T-AOC expression to facilitate oxidative homeostasis. Finally, our results indicated that the Pkm2/Nrf2 pathway is regulated by ECC-BYF III in A549 cells and lung tissue.

Conclusion: These results indicate that ECC-BYF III exerts a strong effective therapeutic effect against cigarette smoke combined with bacteria-induced COPD in rats by activating the Pkm2/Nrf2 signaling pathway and restoring mitochondrial oxidative stress. Although more in vivo animal model research is needed to confirm these findings, this study contributes new data to support the conventional usage of ECC-BYF III.

Keywords: chronic obstructive pulmonary disease, oxidative stress, ECC-BYF III, Pkm2, Nrf2

Introduction

Chronic obstructive pulmonary disease (COPD) is a heterogeneous lung condition characterized by persistent symptoms and airflow limitation.[1] It is an essential cause of chronic morbidity and mortality worldwide. According to the World Health Organization, by 2060, 7 million people with COPD have a mortality rate of 6.9%.[2] It also expected an increment

Received: 8 May 2024
Accepted: 12 August 2024
Published: 24 August 2024

in the mortality rate and cost burden of COPD during the following few decades, owing to global climate change, environmental pollution, and an aging global population.[1]

According to the Global Initiative for Chronic Obstructive Lung Disease (GOLD), oxidative stress is the main pathogenesis of COPD,[1] caused by both endogenous and exogenous oxides, resulting in impaired and/or overwhelming antioxidant defenses. In COPD, oxidative stress is mostly caused by cigarette smoking (CS), which is a major risk factor for illness. However, a noteworthy aspect of COPD is that quitting smoking still does not stop the disease from progressing and oxidative stress in the lung tissue.[3] Thiol antioxidants are widely used in clinical treatment. Examples of these include N-acetylcysteine (NAC), carbocisteine, and erdosteine. Among them, NAC, which has antioxidant characteristics, might raise glutathione levels in the lungs of COPD patients.[4] Nevertheless, multiple 3 studies revealed that NAC had a negligible impact on patients with COPD patient's lung function and quality of life.[5–8] Although animal models have shown that antioxidants are effective in treating COPD, clinical studies are still scarce, only dietary antioxidants, superoxide dismutase (SOD) mimetics, and mitochondria-targeted antioxidants have been noticed.[9] As a result, it is essential to create a drug with a known mode of action that could effectively prevent and manage oxidative stress in COPD.

The mitochondria are the main source of endogenous oxidants. Numerous studies have indicated that mitochondrial dysfunction is a hallmark of COPD.[10–14] Studies have demonstrated that CS can prevent complexes I, II, and III of the mitochondrial respiratory chain by transferring electrons, increasing electron escape, and decreasing mitochondrial membrane potential. In particular, the escaping electrons can combine with oxygen to produce superoxides. Mitochondrial reactive oxygen species (mtROS) build up an oxidative/antioxidant imbalance, mitochondrial DNA damage, mitochondrial apoptosis, and protein structure destruction, eventually resulting in lung tissue damage and accelerating the development of COPD.[15–17] However, no effective mitochondria-targeted antioxidants have been identified in clinical trials.[9]

Pyruvate kinase M2 (Pkm2), in its dimeric state, can translocate to the nucleus as a co-transcriptional activator that regulates gene expression and plays essential roles in energy metabolism, epithelial–mesenchymal transition, oxidative stress, invasion, metastasis, and cell proliferation.[18,19] Related studies have shown that Pkm2 can enter the nucleus and act as a co-activator of nuclear factor E2-related factors (Nrf2), enhancing Nrf2 binding to target gene promoters, such as glutamate cysteine ligase catalytic subunit (GCLC) and glutamate cysteine ligase modifier subunit (GCLM). To resist mitochondrial oxidative stress, Nrf2 increases the synthesis of antioxidant enzymes such as GCLC and GCLM.[20,21] Therefore, activating the Pkm2/Nrf2 signaling pathway may be a crucial strategy for reducing mitochondrial oxidative stress.

Significant advancements have been made in Traditional Chinese Medicine (TCM) therapy for COPD. The Bufei Yishen Formula (BYF; patent ZL.201110117578.1) has been shown to have beneficial effects in the treatment of COPD. Previous studies indicated that BYF could regulate immune function,[22] alleviated lung inflammation,[23] and inhibit oxidative stress response in COPD rats.[24] Due to the complex composition and multiple targets of the formula, the pharmacological mechanism has been challenging to elucidate.[25] Five effective components have been identified from BYF herbal medicines based on vivo and vitro investigations, then combined in a certain ratio to create the effective-component compatibility of BYF III (ECC-BYF III; patent ZL 201811115372.3).[26–28] Traditional Chinese medicine, which emphasizes holistic and synergistic treatment approaches, offers a rich source of potential therapeutics. ECC-BYF III exemplifies this integration, combining multiple active components to target COPD's complex pathology. According to the COPD rat's studies, ECC-BYF III showed a dramatically improvement in lung function, lung histology, a reduction of oxidative stress, inflammatory response and improved airway mucus hypersecretion.[28–31] However the exact method of ECC-BYF III is still vague. Based on the Pkm2/Nrf2 pathway, it is pivotal in regulating cellular responses to oxidative stress, particularly in maintaining mitochondrial integrity. By activating this pathway, ECC-BYF III may offer a targeted approach to mitigating oxidative damage in COPD.

The goal of this study was to investigate how ECC-BYF III controls the Pkm2/Nrf2 pathway in order to understand mitochondrial oxidative damage in COPD. We expect that this study uniquely identifies the Pkm2/Nrf2 pathway as a critical mediator of ECC-BYF III's protective effects against oxidative stress in COPD, a finding that could pave the way for new therapeutic strategies.

Materials and Methods

CSE-Induced Mitochondrial Oxidative Damage Model of A549 Cells

Mainstream cigarette smoke was drawn into a 50 mL syringe and slowly injected into serum-free RPMI Medium 1604 (RPMI 1640). Optical density at 320 nm was measured using a spectrophotometer and adjusted to 1.8–2.0 RPMI 1640. The prepared cigarette smoke extract (CSE) solution was then filtered (0.22 μm) to obtain a 100% CSE solution.

The alveolar epithelial cell line (A549) was purchased from the American Type Culture Collection (ATC, Manassas, VA, USA), and cultured in RPMI 1640 (Solarbio, Science & Technology Co., Ltd., Beijing, China) supplemented with 10% fetal bovine serum (FBS; Gibco, Australia) at 37 °C in a CO_2 humidified incubator. A459 cells were seeded in 6-well plates at a concentration of 1.5×10^5 cells/mL and incubated overnight. The supernatant was discarded, CSE at a final concentration of 10% was added, and cells were incubated for 6, 12, and 24 h. Cells were then collected to prepare cell homogenates.

Effects of Pkm2 Expression Plasmid on CSE-Induced Mitochondrial Oxidative Stress Model of A549 Cells

The Pkm2 expression plasmid was synthesized by Sangon Biotech (Shanghai, China). The pCDH-CMV-puromycin vector was modified to pCDH-CMV-BLAST, and PKM2 cDNA was cloned using standard molecular cloning methods. A549 cells were seeded in 6-well plates at a concentration of 1.5×10^5 cells/mL and incubated overnight. The supernatant was discarded, CSE was added at a final concentration of 10%, and the cells were incubated for 24 h. A549 cells were transfected with 2 μg of the overexpression plasmid or negative control vector using PEI MAX (MW 40,000). For plasmid transfection, cells were cultured with PEI MAX (MW 40,000) and transfected with specific or control plasmids for 24 h. The medium was then replaced with fresh medium and the cells were further cultured for 24 h. The PCDH-Pkm2 sequences used in the present study are listed in Table 1.

Drugs Preparation

ECC-BYF III is composed of five ingredients. Ginsenoside Rh1 (CHB180608) was obtained from Chengdu Chroma Biotechnology Co. Ltd. Astragaloside IV (MUST-17022804), icariin (MUST-16111710), and paeonol (MUST-16071405) were purchased from Chengdu MUST Biotechnology Co., Ltd. Nobietin (HL-20170312) was obtained from Xi'an Huilin Biotechnology Co. Ltd. The contents of these five components, as determined by high-performance liquid chromatography, were not less than 98%. Before use, they were dissolved in a certain proportion of 0.5% carboxymethyl cellulose sodium (CMC-Na) to form a suspension. Acetylcysteine, which served as the positive control drug, was provided by Zambon Pharmaceutical Co., Ltd. (Hainan, China).

Establishment and Treatment of COPD Rat Model

Thirty-two male SPF-grade Sprague-Dawley (SD) rats (250 ± 20 g) were purchased from Beijing Vital River Laboratory Animal Technology Co., Ltd. (Special Pathogen Free, No.110011211105823815). The experimental protocol was reviewed and approved by the Experimental Animal Care and Ethics Committee of the First Affiliated Hospital, Henan University of Traditional Chinese Medicine (Zhengzhou, China; Approval No. YFYD W2019031), and complied with the Regulations on the Administration of Experimental Animals.

After a 7-day adaptive feeding period, 32 rats were randomly divided into four groups: Normal, Model, NAC, and ECC-BYF III, with 8 rats in each group, using the random number table method. The COPD stable phase model was

Table 1 The Sequences of the Pkm2-PACH

Primer	Primer Sequence (5'-3')
F1	GACCTCCATAGAAGATTCTAGAGCCAGCATGGATTACAAAGACGATG
F2	CCATGGATTACAAAGACGATGACGATAAGCAGTGGAGCTCAGAGAGAGG
R1	CGCAGATCCTTCGCGGCCGCGGATCCTCACGGCACAGGAACAACACG

established over a period of 8 weeks through cigarette smoke exposure and bacterial infection. Briefly, the whole body of COPD model rats were exposed to cigarette (China Hongqiqu@filtered cigarettes) smoke twice a day, with a minimum interval of 3 h between the two smoking sessions. The smoke concentration was 3000±500 ppm and each smoking session lasted for 40 min. Additionally, the rats were exposed to Klebsiella pneumoniae once every five days by nasal drip. The bacterial suspension used had a concentration of 6×108 CFU/mL, and each rat was administered 0.1 mL of the suspension (strain number: 46117; obtained from the China Pharmaceutical Bio China Medical Bacteria Preservation Management Center, Institute for Product Control).[32]

From week 9 to week 16, the treatment group consisting of drug-treated COPD model rats received oral administration of ECC-BYF III (dose: 5.5 mg/kg/d, q.d) or NAC (dose: 54 mg/kg/d, q.d). Rats in the normal and model groups were orally administered 0.5% carboxymethylcellulose sodium (CMC-Na) at a volume of 2 mL once daily. The dosages of ECC-BYF III and NAC were determined and adjusted weekly, according to the following formula: $D_{rat} = D_{human} \times (HI_{rat}/ HI_{human}) \times (W_{rat}/ W_{human})^{2/3}$. where D is the dose, HI is the body size index, and W is body weight. At the end of week 16, the rats were euthanized using 2% sodium pentobarbital (40 mg/kg) and tissue samples were collected.

Pulmonary Function Measurement

A whole-body plethysmography (WBP) system (Buxco Inc., Wilmington, North Carolina, USA) was administered every four weeks to measure lung function in unrestrained rats. Relevant continuous ventilation parameters were calculated including tidal volume (Vt) and peak expiratory flow (PEF). A fine PointeTM pulmonary function testing (PFT) system (Buxco Inc., USA) was used to measure the forced vital capacity (FVC), forced expiratory volume at 0.1s (FEV0.1s) and Cdyn of rats.

Histopathology and Immunohistochemistry Analysis

The left lung lobe tissues of the rats were fixed in 10% paraformaldehyde for 72 h, dehydrated, and embedded in paraffin. Paraffin blocks were cut into 4 μm sections and stained with hematoxylin and eosin. Subsequently, the stained tissue sections were observed and photographed using an optical microscope and photography system (Olympus Optical, Japan). Six photographs from each group were selected for the analysis. Six fields of view from each image were randomly selected to count the alveolar septa (Ns), alveoli (Na), and the alveolar area (S). These parameters were calculated using the formulas MLI (μm) = L/Ns and MAN (pieces/mm2) = Na/S to determine the mean alveolar intercept (MLI) and the mean alveolar number (MAN). Additionally, the bronchial wall thickness (BWt) was measured to evaluate pathological changes in the small bronchia.[33,34]

Immunohistochemistry (IHC) was performed to assess the protein expression levels of SOD2. Paraffin-embedded esophageal sections were stained with primary antibodies recognizing SOD2 (1:1000, GeneTex, GTX116093) at 4 °C overnight. After incubation with the primary antibodies, followed by incubation with HRP-conjugated goat anti-rabbit IgG secondary antibody and 3.3'-diaminobenzidine (DAB) were used for the color reaction. The sections were counterstained with hematoxylin. The integral optical densities (IODs) of SOD2 were measured using Image-Pro Plus 6.0, (IPP 6.0) software (Media Cybernetics).

The Activity Antioxidative Enzyme Analysis

An appropriate amount of lung tissue was added at nine times the volume of the PBS. The lung tissue and cell suspension were ground with a tissue disruptor (Servicebio, China) and centrifuged at 12,000 × g at 4 °C for 15 min to obtain a homogenate. Total superoxide dismutase (T-SOD) was determined using a hydroxylamine colorimetric assay kit (A001-1-2, Nanjing Jiancheng Bioengineering Institute, China), total antioxidant capacity (T-AOC) was assayed using a ferric ion reducing antioxidant power (FRAP) colorimetric assay kit (A015-3-1, Nanjing Jiancheng Bioengineering Institute, China), thiobarbituric acid assay kit (A003-1-2, Nanjing Jiancheng Bioengineering Institute, China) was used to measure malondialdehyde (MDA), and glutathione peroxidase (GSH-Px) was determined using a colorimetric method (A005-1-2, Nanjing Jiancheng Bioengineering Institute, China). T-SOD and GSH-Px levels in A549 cells were determined using the method described above. The kits were purchased from Elabscience Biotechnology, Inc. (Wuhan, China). Protein concentration was determined using the BCA method.

Analysis of Mitochondrial Function

The enzymatic activities of mitochondrial complexes I and III in A549 cells and lung tissue were determined using spectrophotometry with kits from Solarbio (Shanghai, China) according to the manufacturer's protocol. Single-cell suspensions of A549 cells were prepared for the assessment of mitochondrial membrane potential using a JC-10 Assay Kit (Solarbio, Shanghai, China). The treated cells were stained with JC-10 and the fluorescence values were measured using a flow cytometer (BD FACSCelesta™, USA). Mitochondria were extracted from lung tissue using a mitochondrial extraction kit (Solarbio, Shanghai, China), the membrane potential of purified mitochondria in lung tissue was detected using the JC-10 Assay Kit (Solarbio, Shanghai, China), and fluorescence values were measured with a fluorescent spectrophotometer.

Quantitative Real-Time PCR

Quantitative real-time PCR (qRT-PCR) was conducted to determine the mRNA expression levels of Pkm2, Nrf2, GCLG, and GCLM in the A549 cells and lung tissues. Total RNA was extracted using the QIAzol® Lysis Reagent (QIAGEN). Reverse transcription was performed using HiScript® II Q RT SuperMix. qRT-PCR was carried out using ChamQ Universal SYBR and specific primers on a Biosystems 7500 instrument; the rat and human primers are shown in Tables 2 and 3. HiScript® II Q RT SuperMix and ChamQ Universal SYBR were obtained from Vazyme Biotech Co. Ltd. Primers were provided by GenScript Biotech Co. Ltd.

Table 2 Rat Primer Sequences for qRT-PCR

Gene	Product Length	Primer	Primer Sequence (5'-3')
GAPDH	76	Forward primer	CCGCATCTTCTTGTGCAGTG
		Reverse primer	TACGGCCAAATCCGTTCACA
Pkm2	120	Forward primer	AGGCTGCCATCTACCACTTG
		Reverse primer	CACTGCAGCACTTGAAGGAG
Nrf2	97	Forward primer	ATTTGTAGATGACCATGAGTCGC
		Reverse primer	GCTATCGAGTGACTGAGCCTG
GCLC	109	Forward primer	CATCGATCACCTTCTGGCAC
		Reverse primer	AAAATGGTCAGACTCGTTGGC
GCLM	112	Forward primer	TTTCCTTGGAGCATTTGCAGC
		Reverse primer	AGCTGCTCCAACTGTGTTTTG

Table 3 Human Primer Sequences for qRT-PCR

Gene	Product Length	Primer	Primer Sequence (5'-3')
GAPDH	226	Forward primer	TTGCGTCGCCAGCCG
		Reverse primer	TTCTCAGCCTTGACGGTGCC
Pkm2	118	Forward primer	ATGTCGAAGCCCCATAGTGAA
		Reverse primer	TGGGTGGTGAATCAATGTCCA
Nrf2	106	Forward primer	CCAGTCAGAAACCAGTGGAT
		Reverse primer	GAATGTCTGCGCCAAAAGCTG

(*Continued*)

Table 3 (Continued).

Gene	Product Length	Primer	Primer Sequence (5'-3')
GCLC	79	Forward primer	GGAGGAAACCAAGCGCCAT
		Reverse primer	CTTGACGGCGTGGATGATGT
GCLM	239	Forward primer	TGTCTTGGAATGCACTGTATCTC
		Reverse primer	CCCAGTAAGGCTGATAATGCTC

Western Blotting

Western blot (WB) analysis was used to evaluate the protein expression levels of Pkm2, Nrf2, GCLC, and GCLM in lung tissues and A549 cells as well as the protein expression levels of Bcl-2, Bax, Cyto-C, and Caspase-3 in A549 cells. Cells were lysed using radioimmunoprecipitation assay lysis buffer supplemented with protease and phosphatase inhibitors. The protein concentration was determined using a BCA protein assay kit (PC0020, Solarbio, Science and Technology Co., Ltd). Protein samples were separated using 10% sodium dodecyl sulfate-polyacrylamide gel electrophoresis and transferred onto polyvinylidene difluoride membranes. Membranes were blocked with 5% skimmed milk in Tris-buffered saline with Tween (TBST) at room temperature for 1 h, followed by overnight incubation with specific primary antibodies, including GAPDH (10494-1-AP, Proteintech), Pkm2 (3198, CST), Nrf2 (GTX1033322, Genetex), GCLC (GTX66057, Genetex), GCLM (GTX114075, Genetex), Bcl-2 (68,103-1-Ig, Proteintech), Bax (50599-2-Ig, Proteintech), Cyto-C (10993-1-AP, Proteintech), and Caspase-3 (82,202-1-RR, Proteintech) at 4 °C. Subsequently, the membranes were incubated with HRP-conjugated secondary antibodies, specifically goat anti-mouse and anti-rabbit antibodies, for 1 hour at room temperature. After washing the membranes three times with TBST, protein bands were visualized using an enhanced chemiluminescence reagent. The intensities of the bands corresponding to the proteins of interest were normalized to the intensity of GAPDH control bands. Grayscale values were analyzed using the ImageJ software.

Statistical Analysis

All data were analyzed using IBM SPSS Statistics for Windows (Version 22.0; IBM Corp., Armonk, NY, USA) and are presented as mean ± standard deviation. Significant differences were determined using one-way ANOVA, followed by the least significant difference method for data with homogeneity of variance, and Dunnett's T3 method for data without homogeneity of variance. The significance level was set at $P < 0.05$. Graphs were generated using GraphPad Prism 10.0.

Results

CSE-Induced Mitochondrial Oxidative Damage

Cigarette smoke is the major cause of COPD, previous studies have shown that cigarette smoke heightens oxidative stress.[35] After treating A549 cells with 10% CSE for 6, 12, and 24 hours, the generation of mtROS was significantly increased, as evidenced by a substantial enhancement in the average fluorescence intensity of red mitochondrial superoxide. The induction of mtROS was most prominent 24 h post-treatment. Furthermore, the mitochondrial membrane potential and activities of mitochondrial respiratory chain complexes I and III were significantly reduced ($P < 0.05$, $P < 0.01$; Figure 1A-E). The effect of decreased mitochondrial respiratory chain complex III enzyme activity was substantially greater at 12 h and 24 h of induction than at 6 h of 10% CSE administration, indicating impaired mitochondrial function. Additionally, exposure to 10% CSE significantly inhibited the activities of antioxidant enzymes T-SOD and GSH-Px ($P < 0.05$, $P < 0.01$; Figure 1F and G). Moreover, the protein expression levels of Caspase-3, Bax, and Cyto C increased, whereas the expression of Bcl-2 decreased ($P < 0.05$; Figure 1H). Importantly, both the mRNA and protein expression of Pkm2, Nrf2, GCLC, and GCLM significantly decreased following 10% CSE treatment. After 24 h of induction with 10% CSE, the decrease in GCLC protein and Pkm2 mRNA expression was significantly greater than that observed after CSE exposure for 6 h. Additionally, the reduction in the mRNA expression of Nrf2, GCLC, and GCLM was significantly more pronounced compared with CSE exposure for 6 and 12 h. ($P < 0.05$, $P < 0.01$; Figure 1I and J).

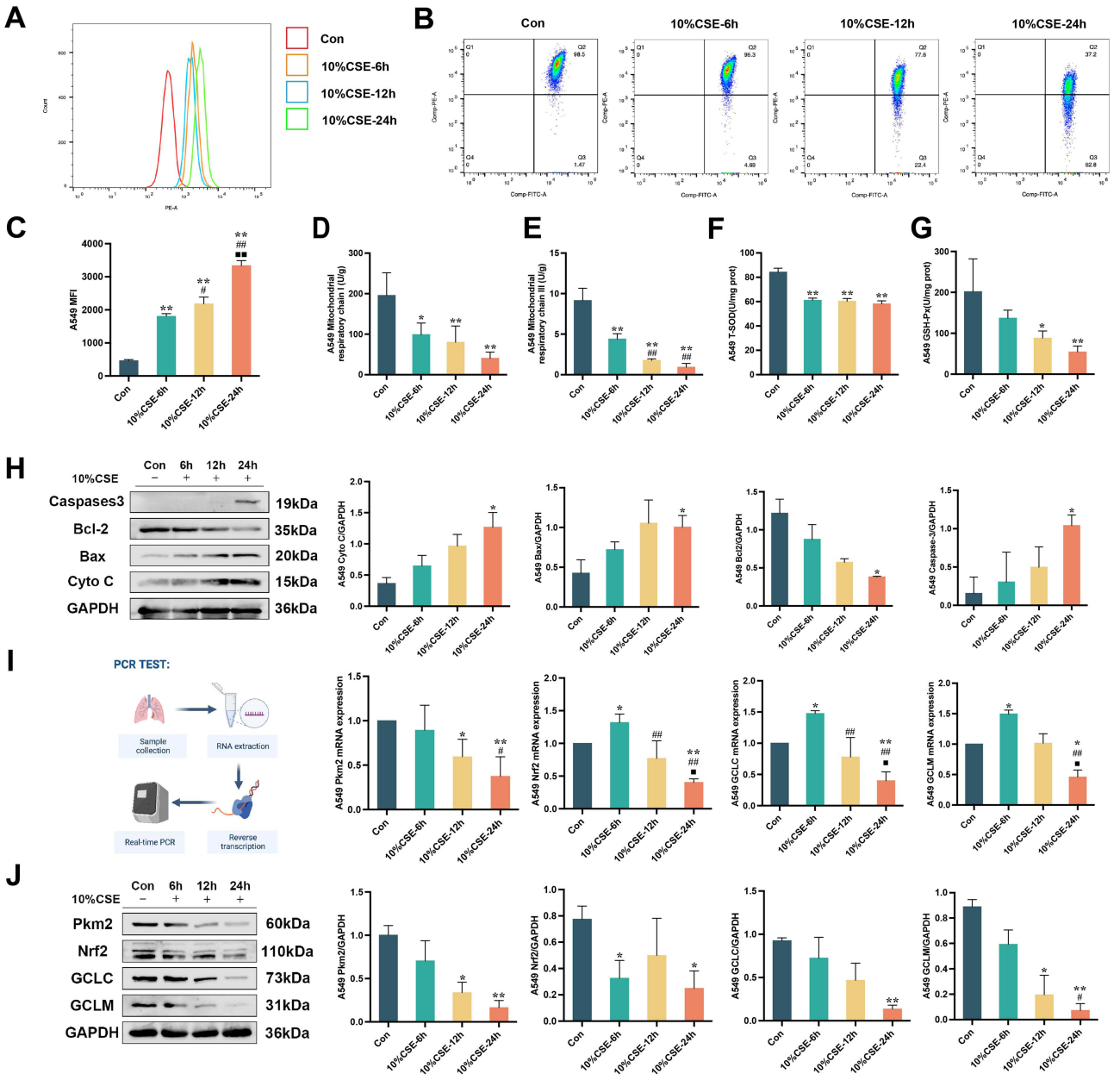

Figure 1 The effects of CSE on mitochondrial oxidative damage and Pkm2/Nrf2 signaling pathway in A549 cells. (**A** and **C**) The effects of 10%CSE induction for 6 hours, 12 hours, and 24 hours on the generation of mROS in A549 cells. (**B**) Inhibition of mitochondrial membrane potential after 10%CSE induction for 6 hours, 12 hours, and 24 hours. (**D** and **E**) Inhibition of mitochondrial respiratory chain complex I and III after 10%CSE induction for 6 hours, 12 hours, and 24 hours. (**F** and **G**) Inhibition of T-SOD and GSH-Px after 10%CSE induction for 6 hours, 12 hours, and 24 hours. (**H**) Western blot analysis for assessing the effects of mitochondrial-related pathway including caspase-3, Bcl-2, Bax, and Cyt-C in A549 cells following 10%CSE induction. (**I**) Quantitative real-time PCR analysis for assessing the effects of Pkm2/Nrf2 signaling pathway including Pkm2, Nrf2, GCLC, and GCLM in A549 cells following 10%CSE induction. (**J**) Western blot analysis for assessing the effects of Pkm2/Nrf2 signaling pathway including Pkm2, Nrf2, GCLC, and GCLM in A549 cells following 10%CSE induction. All data are represented as mean ± SD (n=3). $^{*}P < 0.05$ and $^{**}P < 0.01$ as compared to Con group, $^{\#}P < 0.05$ and $^{\#\#}P < 0.01$ as compared to 10%CSE-6h group, and $^{\blacksquare}P < 0.05$ and $^{\blacksquare\blacksquare}P < 0.01$ as compared to 10%CSE-12h group.

Activation of Pkm2/Nrf2 Protects Mitochondria from Oxidative Damage

Activation of the Pkm2/Nrf2 signaling pathway can effectively inhibit CSE-induced mitochondrial oxidative damage. A549 cells were transfected with Pkm2 expression plasmid for 48 h, followed by 24-hour induction with 10% CSE. Subsequently, cells were collected for analysis. We found that pre-protection with the Pkm2 expression plasmid significantly inhibited mtROS production, improved mitochondrial membrane potential, enhanced the enzyme activity of mitochondrial respiratory chain complexes I and III, and increased the activity of antioxidant enzymes T-SOD and GSH-Px ($P < 0.05$, $P < 0.01$;

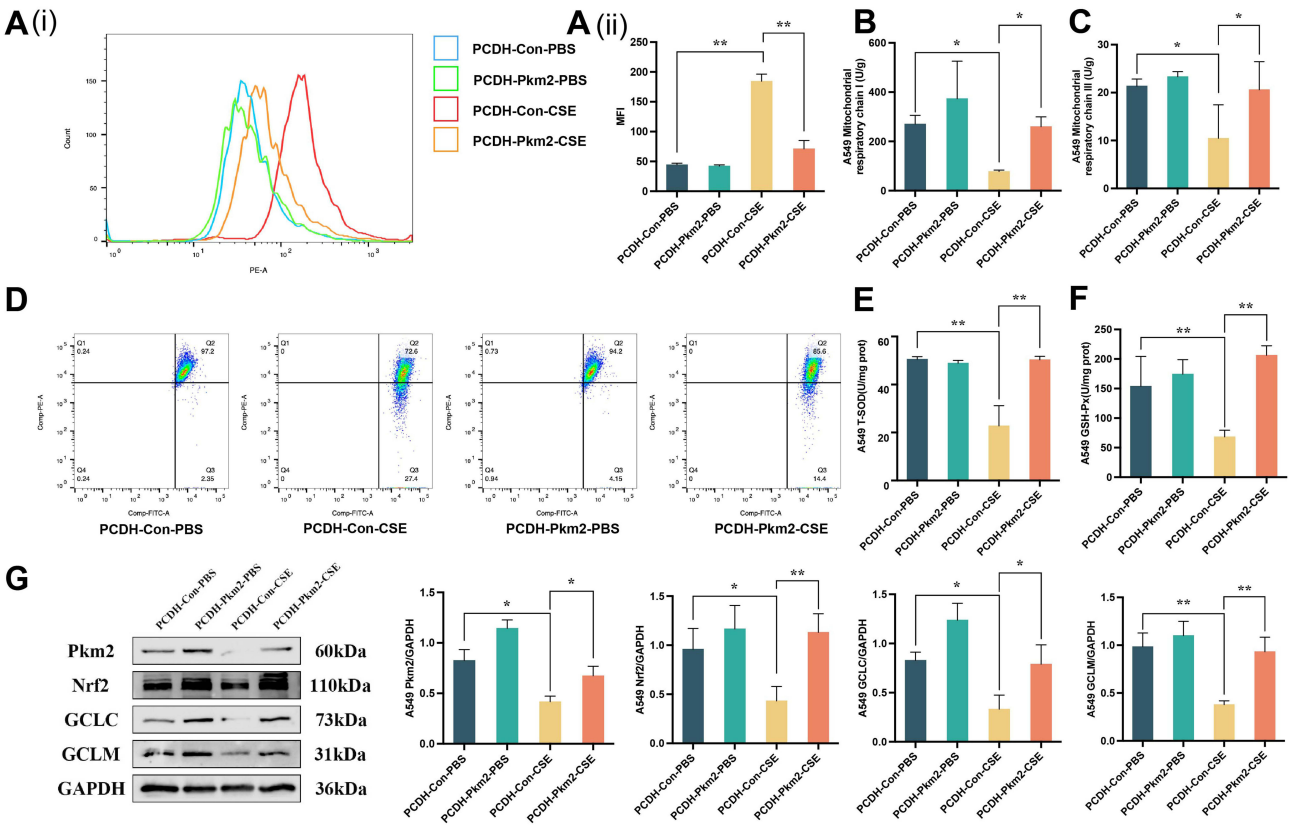

Figure 2 Mitochondria can be protected from oxidative damage by activating the Pkm2/Nrf2 signaling pathway. (**A** (i) and (ii)) The production of mtROS after treated for Pkm2 expression plasmid in A549 cells. (**B**–**D**) Changes in mitochondrial membrane potential, and enzymatic activities of mitochondrial respiratory chain complexes I and III. (**E** and **F**) The activity of T-SOD and GSH-Px with Pkm2 expression plasmid. (**G**) Western blot analysis for assessing the effects of Pkm2/Nrf2 signaling pathway including Pkm2, Nrf2, GCLC, and GCLM in A549 cells following Pkm2 expression plasmid transfection. All data are represented as mean ± SD (n=3). * and ** indicate $P < 0.05$ and $P < 0.01$.

Figure 2A–F). Western blot analysis was performed to assess the impact of Pkm2 overexpression on the Pkm2/Nrf2 signaling pathway. The results revealed that Pkm2 overexpression effectively activated the Pkm2/Nrf2 signaling pathway and prevented the decline in the downstream antioxidant proteins GCLC and GCLM ($P < 0.05$, $P < 0.01$; Figure 2G).

Effect of ECC-BYF III on Pulmonary Function and Histopathological Changes in COPD Rats

The COPD rat model was adopted from previous studies.[32] Figure 3A shows the detailed experimental design of this study. COPD rats received i.g. treatment with ECC-BYF III or NAC per mouse per day for eight weeks. In COPD rats, Vt, PEF, FVC, and FEV0.1s were significantly reduced, whereas airway resistance was increased. At the same time, increased Cdyn indicates increased lung compliance and emphysema in the lungs ($P < 0.05$, $P < 0.01$; Figure 3B–F). Treatment with ECC-BYF III and NAC significantly improved lung function. Figure 3G illustrates the histopathological alterations observed in COPD rats, including alveolar and bronchial thickening, emphysema, and infiltration of inflammatory cells. H&E staining revealed an intact alveolar structure in the normal group with no alveolar rupture or fusion. The small airway structure of the lung was normal with no thickening of the airway wall or inflammatory cell infiltration around the airway. In the Model group, alveolar rupture and fusion were evident, resulting in the formation of oval-shaped alveolar cavities. The alveolar cavity per unit area was reduced, airway wall was thickened, and inflammatory infiltration around the airway was notable. In the ECC-BYF III and NAC groups, alveolar rupture was reduced, alveolar space per unit area was increased, airway wall thickness was decreased, and inflammatory cell infiltration around the airway was alleviated. Quantitative analysis of MAN, MLI, and BWt in the sampled sections demonstrated that increases in MLI and BWt were accompanied by decreases in the MAN. Moreover, ECC-BYF III exhibited a better effect than NAC in reducing MLI and increasing MAN ($P < 0.05$, $P < 0.01$; Figure 3H–J).

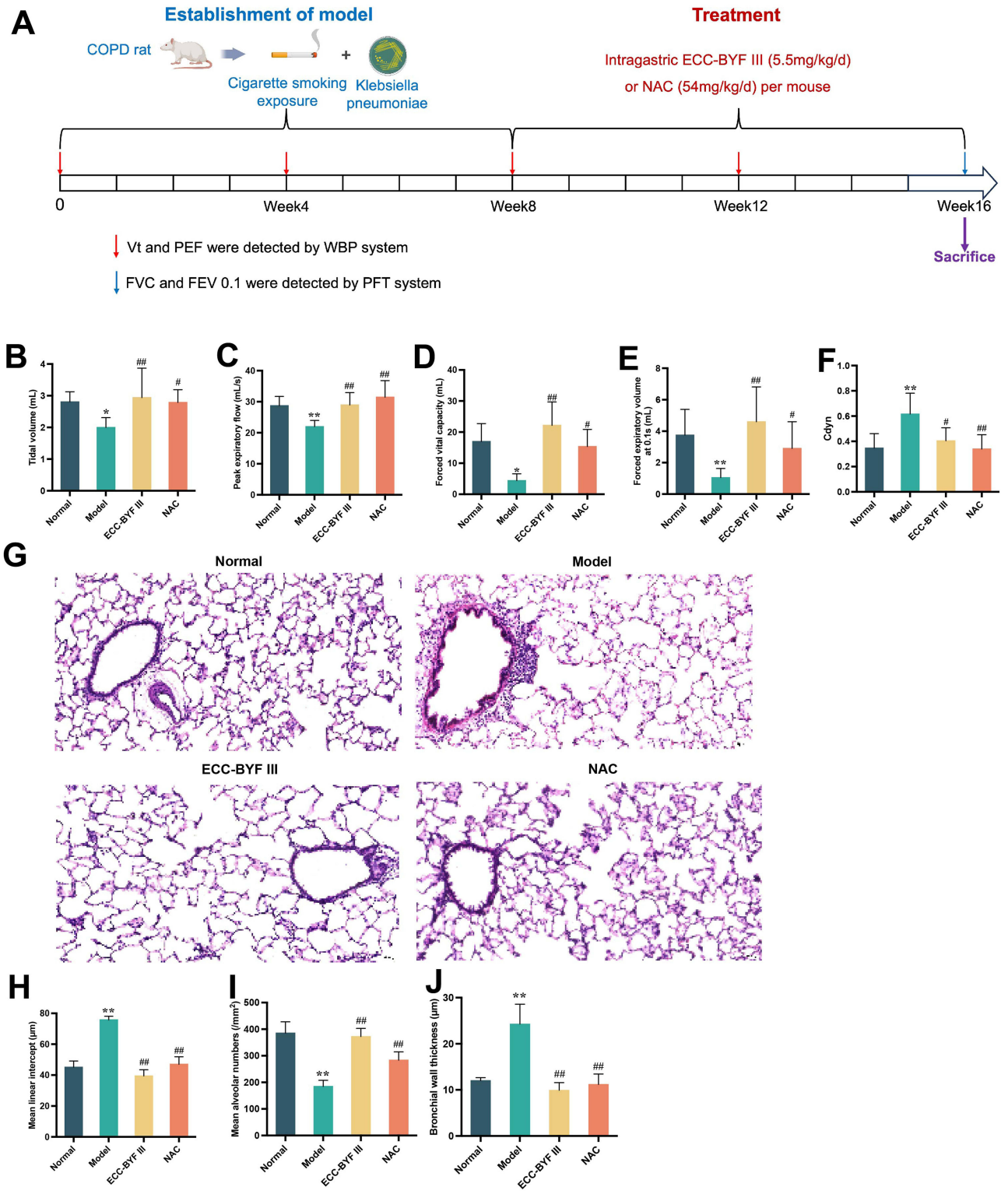

Figure 3 Effects of ECC-BYF III on lung function and lung histopathology in COPD rats. (**A**) Establishment process and treatment measures of COPD rat model induced by smoking and Klebsiella pneumoniae. (**B**–**F**) Tidal volume, peak expiratory flow, forced vital capacity, forced expiratory volume at 0.1s and Cdyn of rats. (**G**) H and E pathological section of lung (200×). (**H**–**J**) Mean alveolar number, mean alveolar intercept, and bronchial wall thickness. All data are represented as mean ± SD (n=6~8). *P < 0.05 and **P < 0.01 as compared to Normal group, $^{\#}P$ < 0.05 and $^{\#\#}P$ < 0.01 as compared to Model group.

Effects of ECC-BYF III on Oxidative Stress in Lung Tissue of COPD Rats

Following the administration of ECC-BYF III and NAC, the activities of T-SOD, T-AOC, and GSH-Px significantly increased, while the expression of MDA decreased ($P < 0.05$, $P < 0.01$; Figure 4A–D).

Effects of ECC-BYF III on Mitochondrial Function in Lung Tissue of COPD Rats

In this study, the ultrastructure of the mitochondria in lung tissues and the activity of the enzymes that form the mitochondrial respiratory chain complex were analyzed. As shown in Figure 5A, the control group exhibited type II alveolar epithelial cells with intact structures and neatly arranged villi. The mitochondria were abundant, large, and normal in shape. The boundary with the surrounding area was clear, and mitochondrial cristae were clearly visible. In the Model group, the number of mitochondria decreased and appeared smaller in volume. Mitochondrial pyknosis and swelling were observed; however, the boundary with the surrounding area was unclear. The mitochondrial cristae appear blurred. The number and volume of mitochondria increased in the ECC-BYF III and NAC groups. Mitochondria exhibited a normal shape, clear boundaries with the surrounding area, and clear cristae. SOD2, an important antioxidant enzyme in the mitochondrial matrix, was dramatically reduced in the lung tissue of COPD rats, whereas ECC-BYF III and NAC significantly boosted SOD2 protein synthesis in the lung tissue ($P < 0.01$, Figure 5B and C). The activities of the mitochondrial respiratory chain complex I and III enzymes in the model group were also considerably decreased ($P < 0.01$) in comparison to the mitochondrial membrane potential of the normal group. Nevertheless, the ECC-BYF III and NAC treatment groups significantly outperformed the model group in terms of mitochondrial membrane potential and activity of respiratory chain complexes I and III of the mitochondria. ECC-BYF III therapy increased the activity of mitochondrial respiratory chain complex I compared to NAC ($P < 0.05$, $P < 0.01$; Figure 5D-F).

ECC-BYF III Up-Regulates Pkm2/Nrf2 Signaling Pathway in COPD Rats

To combat oxidative stress, ECC-BYF III activates the Pkm2/Nrf2 signaling pathway. We investigated the expression of proteins and mRNAs related to the Pkm2/Nrf2 signaling pathway. Pkm2, Nrf2, GCLC, and GCLM mRNA and protein expression in the lung tissue of COPD rats treated with ECC-BYF III and NAC were significantly higher than those in the model group ($P < 0.01$, $P < 0.05$; Figure 6A–I).

Discussion

COPD is a significant public health issue, with high morbidity and mortality rates. In recent years, significant advancements have been made in the treatment of COPD by using traditional Chinese medicine. Its therapeutic advantages have been widely accepted. BYF, consisting of 12 traditional Chinese medicinal herbs, has demonstrated effective improvement in the clinical symptoms of COPD patients, including improvements in clinical symptoms, reduced rate of deterioration in lung function, and reduced frequency of acute exacerbations.[36,37] However, due to the complex composition of traditional Chinese medicine compounds, it is challenging to elucidate the specific mechanisms of action. To construct ECC-BYF III, the effective chemicals icariin, astragaloside IV, nobiletin, ginsenoside Rh1, and paeonol

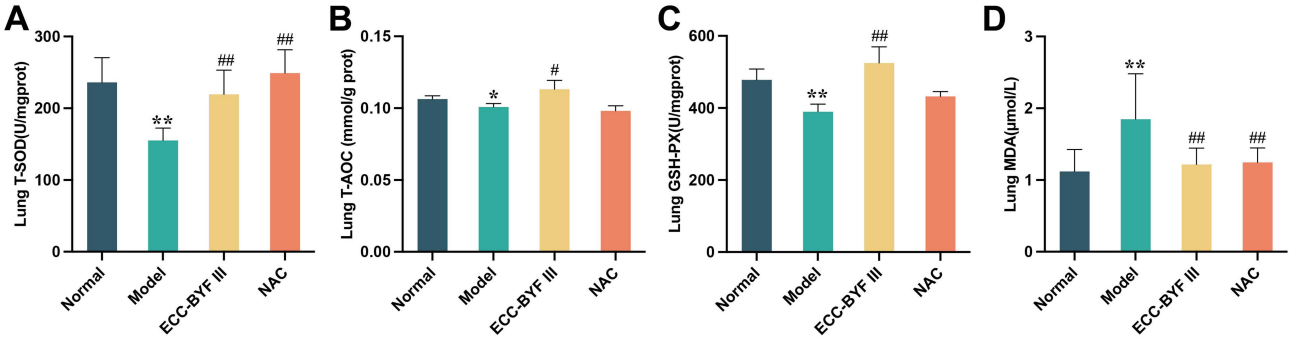

Figure 4 Effects of ECC-BYF III on oxidative stress-related indicators in lung tissue of COPD rats. (**A**) T-SOD, (**B**) T-AOC, (**C**) GSH-Px, (**D**) MDA. All data are represented as mean ± SD (n=6~8). *$P < 0.05$ and **$P < 0.01$ as compared to Normal group, #$P < 0.05$ and ##$P < 0.01$ as compared to Model group.

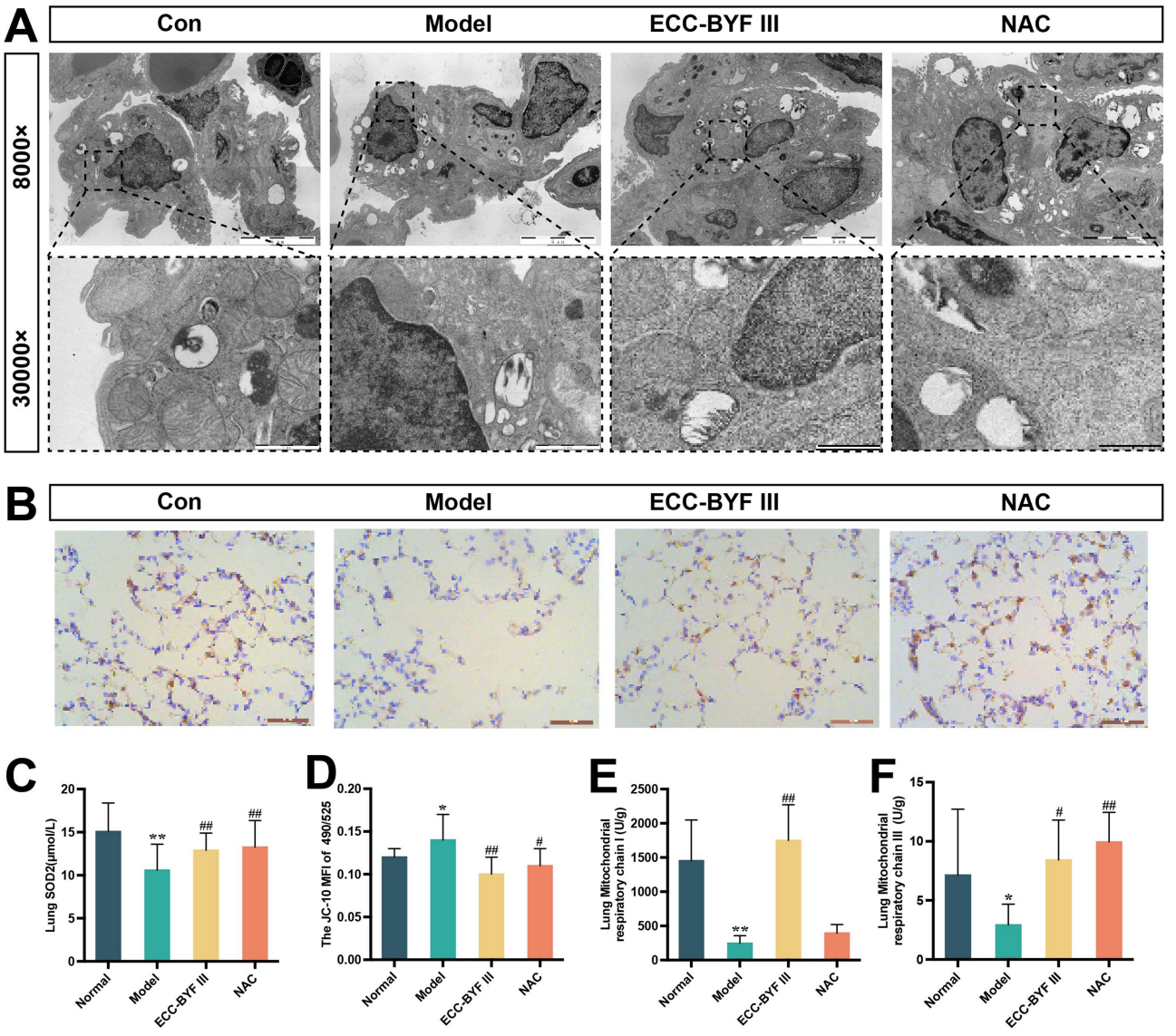

Figure 5 Effects of ECC-BYF III on mitochondrial function-related indicators in lung tissue of COPD rats. (**A**) The integrity of mitochondrial ultrastructure in lung tissue. (**B**) SOD2 immuno-histochemical photomicrographs (200×). (**C**) SOD2 quantification analysis. (**D**–**F**) mitochondrial membrane potential, mitochondrial respiratory chain complexes I and III. All data are represented as mean ± SD (n=6~8). *P < 0.05 and **P < 0.01 as compared to Normal group, $^{\#}P$ < 0.05 and $^{\#\#}P$ < 0.01 as compared to Model group.

from BYF were selected and mixed in a specific ratio.[28,33] In this study, ECC-BYF III effectively improved lung function, lung histopathology, oxidative stress, and impaired mitochondrial function in COPD rats, which were found to be associated with regulation of the Pkm2/Nrf2 signaling pathway.

Cigarette smoking (CS) is an important environmental risk factor for COPD. CS has a higher prevalence of respiratory symptoms and lung abnormalities, a greater annual rate of decline in FEV1, and a greater COPD mortality rate than non-smokers.[38] CS indirectly encourages oxidative stress by reducing the action of important endogenous antioxidant mechanisms, such as the enzymes superoxide dismutase (SOD), glutathione, and Nrf2. Increased oxidative stress, a key pathogenic factor in COPD, can cause aberrant activation of pro-inflammatory pathways and epigenetic modifications such as DNA methylation, histone modification, and altered expression of non-coding RNAs.[39] Patients with acute exacerbation of COPD have been found to exhibit significantly lower levels of the antioxidant glutathione and higher levels of oxidative stress in bronchial lavage fluid (BALF) compared to patients with stable COPD.[40] Oxidative markers such as hydrogen peroxide, nitric oxide, and myeloperoxidase have been found to increase in the exhaled breath or exhaled breath condensate of COPD patients, indicating the presence

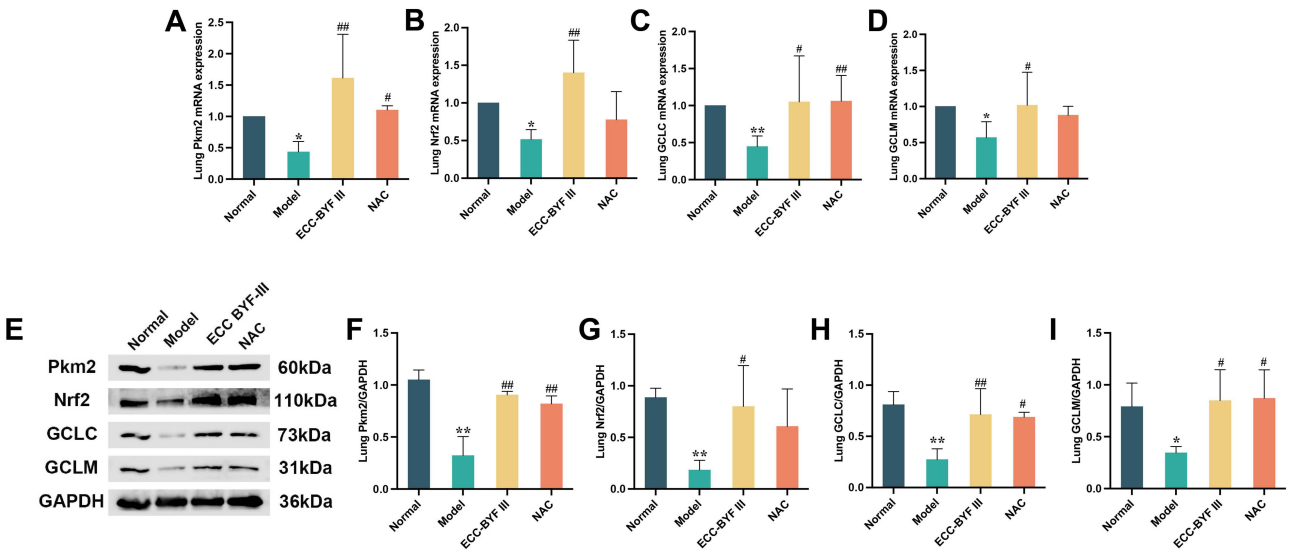

Figure 6 Effects of ECC-BYF III on Pkm2/Nrf2 signaling pathway in lung tissue of COPD rats. (**A**–**D**) Pkm2, Nrf2, GCLC and GCLM mRNA expression in lung tissue; (**E**–**I**) Pkm2, Nrf2, GCLC and GCLM levels as assessed by Western blot. All data are represented as mean ± SD (n=3). $^{*}P < 0.05$ and $^{**}P < 0.01$ as compared to Normal group, $^{\#}P < 0.05$ and $^{\#\#}P < 0.01$ as compared to Model group.

of oxidative stress in the lungs.[41] Reduced levels of antioxidants in lung tissue are associated with worsening lung function in COPD, and antioxidant supplementation has been shown to reduce the risk of COPD by 10% and decrease carbonyl stress in lung tissue.[42,43] Indeed, our studies found that oxidative stress occurred in COPD rats and CSE-induced A549 cells, such as decreased T-SOD and GSH-Px activities, and increased MDA level significantly. ECC-BYF III suppressed pulmonary function reduction and histopathological changes, while improving oxidative stress in rats. Thus, ECC-BYF III exerted a distinct effect on COPD rats by ameliorating oxidative stress in lung tissue.

Related research has shown that the mitochondria are the primary source of endogenous oxidative stress. The mitochondrial respiratory chain components, including complex I, coenzyme Q, complex III, cytochrome C, and complex IV, sequentially transfer NADH and electrons to oxygen through mitochondrial ATP synthases to generate ATP, which provides energy to organisms. However, this process also leads to the production of ROS.[44] A lot of evidence indicates that mitochondria is the primary source of intracellular ROS, with approximately 90% of ROS was generated from mitochondria.[45] mtROS is one type of mitochondrial oxidant. Its production rate is interdependent on the mitochondrial membrane potential and the activity of mitochondrial respiratory chain complexes.[46] Breathing difficulty leads to decreased enzyme activity of the respiratory chain complex, causing increment of electron leakage and the expression of uncoupling proteins, which disrupt the electron concentration gradient across the inner mitochondrial membrane, leading to reduced mitochondrial membrane potential and increased mtROS production.[47] Intracellular antioxidant defense mechanisms counteract ROS production to maintain redox balance and protect lung cells. However, in COPD, the levels of several endogenous antioxidants, such as superoxide dismutase and glutathione peroxidase, are reduced, thereby amplifying oxidative stress in the lungs. Excessive oxidants result in the generation of reactive hydroxyl groups through lipid peroxidation and sugar and sugar oxidation, leading to the formation of protein hydroxylated aldehydes, for instance malondialdehyde.[48] Protein hydroxylation is increased in the lungs of smokers and COPD patients and is correlated with disease severity.[49] In this study, we first discovered that CSE-induced A549 cells had mitochondrial oxidative damage, which was primarily reflected in the increase of mitochondrial superoxide generation, the decrease of mitochondrial respiratory chain complex enzyme activity and mitochondrial membrane potential. Obvious mitochondrial ultrastructural damage was observed in the lung tissues of rats with COPD. Fortunately, ECC-BYF III could considerably mitigate structural damage to the mitochondria and protect mitochondrial function in the lung tissue of COPD rats. Therefore, the effect of ECC-BYF III on oxidative stress in COPD may be achieved by protecting the mitochondrial function.

Pyruvate kinase (PK) is a glycolytic enzyme that exists in its dimeric form Pkm2. There are four isoforms of pyruvate kinase, L, R, M1, and M2.[50] Pkm2 act as transcriptional activators of Nrf2 and enhance its expression of Nrf2. Nrf2

translocates into the nucleus and binds to antioxidant response elements (ARE) to activate the Nrf2/ARE signaling pathway, which promotes the production of downstream antioxidant enzymes. Nrf2, as a transcriptional activator, translocates to the nucleus and promotes the expression of multiple antioxidant genes.[51] Under normal conditions, inactive Nrf2 forms a complex with KEAP1 in the cytoplasm. Upon activation, Nrf2 dissociates from KEAP1, translocated to the nucleus, and binds to antioxidant response elements (AREs) to enhance the expression of target genes such as NQO1 and glutathione.[52] Emphysema caused by cigarette smoke can be prevented and lung oxidation defense system greatly enhanced by activating the Nrf2 signaling pathway. Thus, Pkm2/Nrf2 signaling pathway participates in the regulation of mitochondrial oxidative stress.[53,54] CSE often induces damage to mitochondrial function through oxidative stress, which in turn exacerbates the overall oxidative stress in the body.[55] The data from this experiment demonstrate that Pkm2 and Nrf2 were significantly down-regulated in a CSE-induced mitochondrial oxidative damage model, indicating the inhibition of Pkm2/Nrf2 signaling pathway under mitochondrial oxidative stress. However, overexpression of Pkm2 significantly increased the expression of Nrf2 and its downstream targets GCLC and GCLM, effectively protecting against CSE-induced mitochondrial oxidative damage. These findings highlight the importance of activating the Pkm2/Nrf2 signaling pathway to protect the mitochondria from oxidative stress. In this study, we observed that treatment with ECC-BYF III increased the expression of Pkm2, Nrf2, and their downstream targets GCLC and GCLM in lung tissue.

Conclusions

These findings suggest that ECC-BYF III exerts therapeutic effects in COPD by activating the Pkm2/Nrf2 signaling pathway to protect mitochondria from oxidative damage, as shown in Figure 7.

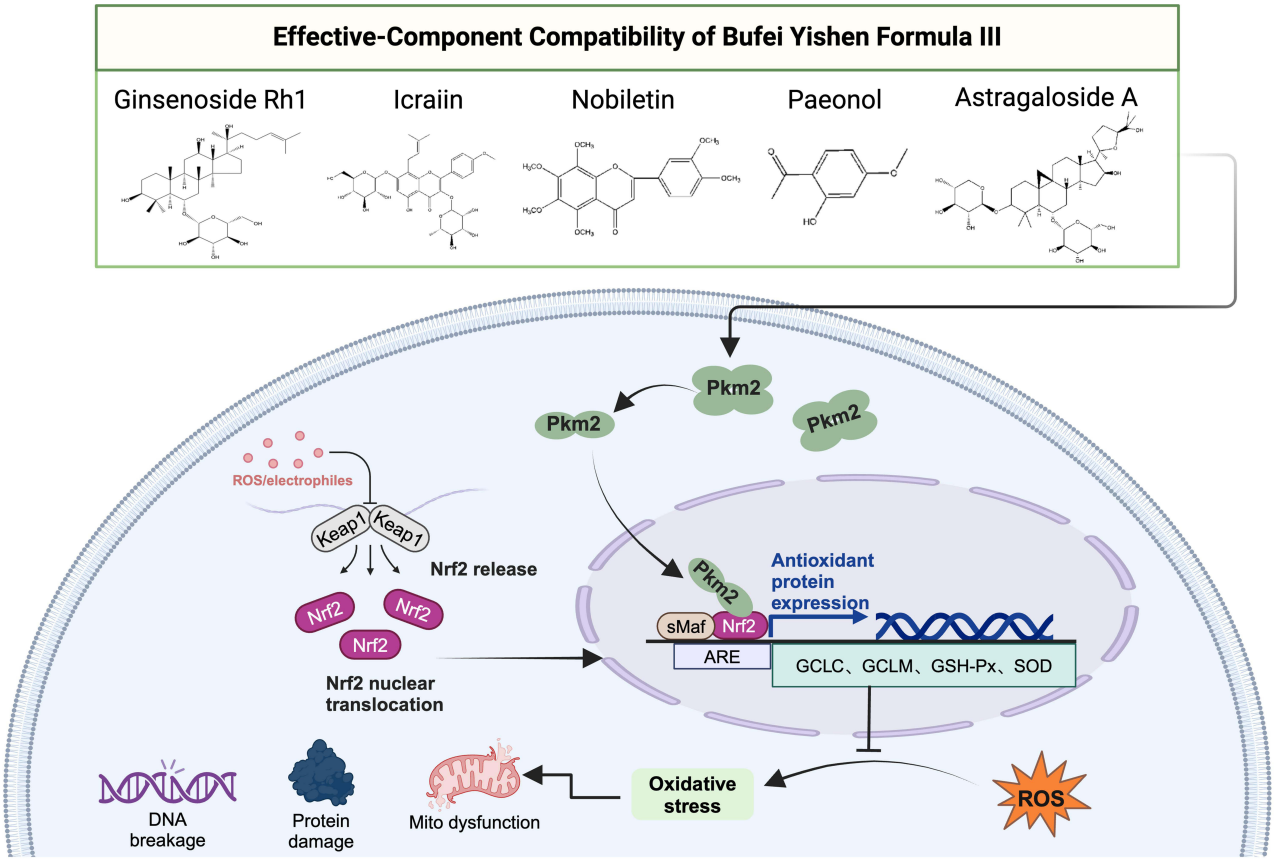

Figure 7 Schematic diagram of ECC-BYF III regulates Pkm2/Nrf2 signaling pathway.

Abbreviations

COPD, Chronic obstructive pulmonary disease; GOLD, Global initiative for Chronic Obstructive Lung Disease; CS, Cigarette smoking; mtROS, mitochondrial reactive oxygen species; Pkm2, Pyruvate kinase M2; Nrf2, nuclear factor E2-related factors; GCLC, glutamate cysteine ligase catalytic subunit; GCLM, glutamate cysteine ligase modifier subunit; BYF, Bufei Yishen Formula; ECC-BYF III, effective-component compatibility of BYF III; Vt, tidal volume; PEF, peak expiratory flow; FVC, forced vital capacity; FEV0.1s, Forced expiratory volume at 0.1s; MLI, mean alveolar intercept; MAN, mean alveolar number; BWt, bronchial wall thickness; T-SOD, Total superoxide dismutase; T-AOC, Total antioxidant capacity; MDA, malondialdehyde; GSH-Px, Glutathione peroxidase.

Data Sharing Statement

Data supporting the findings of this study are available from the corresponding author upon reasonable request.

Ethics Approval and Informed Consent

This study was reviewed and approved by the Experimental Animal Welfare Ethics Review Committee of the First Affiliated Hospital of the Henan University of Chinese Medicine (No.: YFYDW2019031).

Acknowledgments

We thank the Electron Microscope Center of Henan University of Chinese Medicine for their wonderful collaboration and patient support.

Author Contributions

All authors made a significant contribution to the work reported, whether that is in the conception, study design, execution, acquisition of data, analysis and interpretation, or in all these areas; took part in drafting, revising or critically reviewing the article; gave final approval of the version to be published; have agreed on the journal to which the article has been submitted; and agree to be accountable for all aspects of the work.

Funding

This study was financially supported by the National Natural Science Foundation of China (82074406 and 81973822) and the Foundation of the Department of Science and Technology of HeNan Province (No. 232102311215).

Disclosure

The authors report no conflicts of interest in this work.

References

1. Goblal Initiative for Chronic Obstructive Lung Disease. Global strategy for the diagnosis, management, and Prevention of Chronic Obstructive Pulmonary Disease. GOLD REPORT [EB/OL]; 2022. Available from: https://goldcopd.org/2022-gold-reports/. Accessed August 14,2024
2. World Health Organization. Key Facts on COPD.Available from: https://www.who.int/news-room/fact-sheets/detail/chronic-obstructive-pulmonary-disease-(copd). Accessed August 14, 2024.
3. Louhelainen N, Rytilä P, Haahtela T, et al. Persistence of oxidant and protease burden in the airways after smoking cessation. *BMC Pulm Med*. 2009;9(1):25. doi:10.1186/1471-2466-9-25
4. Biswas SK, Rahman I. Environmental toxicity, redox signaling and lung inflammation: the role of glutathione. *Mol Aspects Med*. 2009;30(1–2):60–76. doi:10.1016/j.mam.2008.07.001
5. Grandjean EM, Berthet P, Ruffmann R, et al. Efficacy of oral long-term N-acetylcysteine in chronic bronchopulmonary disease: a meta-analysis of published double-blind, placebo-controlled clinical trials. *Clin Ther*. 2000;22(2):209–221. doi:10.1016/S0149-2918(00)88479-9
6. Zheng JP, Wen FQ, Bai CX, et al. Twice daily N-acetylcysteine 600 mg for exacerbations of chronic obstructive pulmonary disease (PANTHEON): a randomised, double-blind placebo-controlled trial. *Lancet Respir Med*. 2014;2(3):187–194. doi:10.1016/S2213-2600(13)70286-8
7. Decramer M, Rutten-van Mölken M, Dekhuijzen PN, et al. Effects of N-acetylcysteine on outcomes in chronic obstructive pulmonary disease (Bronchitis Randomized on nac cost-utility study, BRONCUS): a randomised placebo-controlled trial. *Lancet*. 2005;365(9470):1552–1560. doi:10.1016/S0140-6736(05)66456-2
8. Poole P, Sathananthan K, Fortescue R. Mucolytic agents versus placebo for chronic bronchitis or chronic obstructive pulmonary disease. *Cochrane Database Syst Rev*. 2019;5(5):Cd001287. doi:10.1002/14651858.CD001287.pub6
9. Barnes PJ. Oxidative stress-based therapeutics in COPD. *Redox Biol*. 2020;33:101544. doi:10.1016/j.redox.2020.101544

10. Hoffmann RF, Zarrintan S, Brandenburg SM, et al. Prolonged cigarette smoke exposure alters mitochondrial structure and function in airway epithelial cells. *Respir Res*. 2013;14(1):97. doi:10.1186/1465-9921-14-97
11. van der Toorn M, Slebos D-J, de Bruin HG, et al. Cigarette smoke-induced blockade of the mitochondrial respiratory chain switches lung epithelial cell apoptosis into necrosis. *Am J Physiol Lung Cell Mol Physiol*. 2007;292(5):L1211–1218. doi:10.1152/ajplung.00291.2006
12. Mizumura K, Cloonan SM, Nakahira K, et al. Mitophagy-dependent necroptosis contributes to the pathogenesis of COPD. *J Clin Invest*. 2014;124 (9):3987–4003. doi:10.1172/JCI74985
13. Giordano L, Farnham A, Dhandapani PK, et al. Alternative oxidase attenuates cigarette smoke-induced lung dysfunction and Tissue Damage. *Am J Respir Cell Mol Biol*. 2019;60(5):515–522. doi:10.1165/rcmb.2018-0261OC
14. Li X, Zhang Y, Yeung SC, et al. Mitochondrial transfer of induced pluripotent stem cell-derived mesenchymal stem cells to airway epithelial cells attenuates cigarette smoke-induced damage. *Am J Respir Cell Mol Biol*. 2014;51(3):455–465. doi:10.1165/rcmb.2013-0529OC
15. Zhao Q, Liu J, Deng H, et al. Targeting Mitochondria-Located circRNA SCAR alleviates Nash via reducing mROS output. *Cell*. 2020;183 (1):76–93. doi:10.1016/j.cell.2020.08.009
16. Shi T, Dansen TB. Reactive oxygen species induced p53 activation: DNA damage, redox signaling, or both? *Antioxid Redox Signal*. 2020;33 (12):839–859. doi:10.1089/ars.2020.8074
17. McGuinness AJ, Sapey E. Oxidative stress in COPD: sources, markers, and potential mechanisms. *J Clin Med*. 2017;6(2):21. doi:10.3390/jcm6020021
18. Wong N, De Melo J, Tang D. PKM2, a central point of regulation in cancer metabolism. *Int J Cell Biol*. 2013;2013:242513. doi:10.1155/2013/242513
19. Wu S, Le H. Dual roles of PKM2 in cancer metabolism. *Acta Biochim Biophys Sin (Shanghai)*. 2013;45(1):27–35. doi:10.1093/abbs/gms106
20. Coaxum SD, Tiedeken J, Garrett-Mayer E, et al. The tumor suppressor capability of p53 is dependent on non-muscle myosin IIA function in head and neck cancer. *Oncotarget*. 2017;8(14):22991–23007. doi:10.18632/oncotarget.14967
21. Teskey G, Abrahem R, Cao R, et al. Glutathione as a marker for human disease. *Adv Clin Chem*. 2018;87:141–159.
22. Zhao P, Li JS, Tian YG, et al. Restoring Th17/Treg balance via modulation of STAT3 and STAT5 activation contributes to the amelioration of chronic obstructive pulmonary disease by Bufei Yishen formula. *J Ethnopharmacol*. 2018;217:152–162. doi:10.1016/j.jep.2018.02.023
23. Tian YG, Li Y, Li JS, et al. Bufei Yishen granules combined with acupoint sticking therapy suppress inflammation in chronic obstructive pulmonary disease rats: via jnk/p38 signaling pathway. *Evid Based Compl Alternat Med*. 2017;2017(1):1768243. doi:10.1155/2017/1768243
24. Li Y, Tian YG, Li JS, et al. Bufei Yishen granules combined with acupoint sticking therapy suppress oxidative stress in chronic obstructive pulmonary disease rats: via regulating peroxisome proliferator-activated receptor-gamma signaling. *J Ethnopharmacol*. 2016;193:354–361. doi:10.1016/j.jep.2016.08.027
25. Li JS, Zhao P, Yang LP, et al. System biology analysis of long-term effect and mechanism of Bufei Yishen on COPD revealed by system pharmacology and 3-omics profiling. *Sci Rep*. 2016;6(1):25492. doi:10.1038/srep25492
26. Li JS, Liu XF, Dong HR, et al. Effective-constituent compatibility-based analysis of Bufei Yishen formula, a traditional herbal compound as an effective treatment for chronic obstructive pulmonary disease. *J Integr Med*. 2020;18(4):351–362. doi:10.1016/j.joim.2020.04.004
27. Li JS, Ma JD, Tian YG, et al. Effective-component compatibility of Bufei Yishen formula II inhibits mucus hypersecretion of chronic obstructive pulmonary disease rats by regulating EGFR/PI3K/mTOR signaling. *J Ethnopharmacol*. 2020;257:112796. doi:10.1016/j.jep.2020.112796
28. Liu L, Qin YQ, Cai ZH, et al. Effective-components combination improves airway remodeling in COPD rats by suppressing M2 macrophage polarization via the inhibition of mTORC2 activity. *Phytomedicine*. 2021;92:153759. doi:10.1016/j.phymed.2021.153759
29. Jin FL, Zhang LX, Chen K, et al. Effective-component compatibility of bufei yishen formula iii combined with electroacupuncture suppresses inflammatory response in rats with chronic obstructive pulmonary disease via regulating sirt1/nf-κb signaling. *Biomed Res Int*. 2022;2022:3360771. doi:10.1155/2022/3360771
30. Liu Y, Zhang LX, Tian YG, et al. Effective characteristics of effective-component compatibility of Bufei Yishen Formula combined with acupuncture in COPD rats based on the onset time and long-term effects. *China J Tradition Chinese Med Pharm*. 2023;37(10):5664–5670.
31. Xu KX, Ma JD, Lu RL, et al. Effective-compound combination of Bufei Yishen formula III combined with ER suppress airway mucus hypersecretion in COPD rats: via EGFR/MAPK signaling. *Biosci Rep*. 2023;43(11):BSR20222669. doi:10.1042/BSR20222669
32. Li Y, Li SY, Li JS, et al. A rat model for stable chronic obstructive pulmonary disease induced by cigarette smoke inhalation and repetitive bacterial infection. *Biol Pharm Bull*. 2012;35(10):1752–1760. doi:10.1248/bpb.b12-00407
33. Li MY, Qin YQ, Tian YG, et al. Effective-component compatibility of Bufei Yishen formula III ameliorated COPD by improving airway epithelial cell senescence by promoting mitophagy via the NRF2/PINK1 pathway. *BMC Pulm Med*. 2022;22(1):434. doi:10.1186/s12890-022-02191-9
34. Zhang LX, Tian YG, Zhao P, et al. Electroacupuncture attenuates pulmonary vascular remodeling in a rat model of chronic obstructive pulmonary disease via the VEGF/PI3K/Akt pathway. *Acupunct Med*. 2022;40(4):389–400. doi:10.1177/09645284221078873
35. Sun X, Feng XL, Zheng DD, et al. Ergosterol attenuates cigarette smoke extract-induced COPD by modulating inflammation, oxidative stress and apoptosis in vitro and in vivo. *Clin Sci (Lond)*. 2019;133(13):1523–1536. doi:10.1042/CS20190331
36. Li JS, Li SY, Xie Y, et al. The effective evaluation on symptoms and quality of life of chronic obstructive pulmonary disease patients treated by comprehensive therapy based on traditional Chinese medicine patterns. *Complement Ther Med*. 2013;21(6):595–602. doi:10.1016/j.ctim.2013.09.006
37. Li SY, Li JS, Wang MH, et al. Effects of comprehensive therapy based on traditional Chinese medicine patterns in stable chronic obstructive pulmonary disease: a four-center, open-label, randomized, controlled study. *BMC Compl Altern Med*. 2012;12(1):197. doi:10.1186/1472-6882-12-197
38. Kohansal R, Martinez-Camblor P, Agustí A, et al. The natural history of chronic airflow obstruction revisited: an analysis of the Framingham offspring cohort. *Am J Respir Crit Care Med*. 2009;180(1):3–10. doi:10.1164/rccm.200901-0047OC
39. Rangasamy T, Cho CY, Thimmulappa RK, et al. Genetic ablation of Nrf2 enhances susceptibility to cigarette smoke-induced emphysema in mice. *J Clin Invest*. 2004;114(9):1248–1259. doi:10.1172/JCI200421146
40. Fratta Pasini AM, Stranieri C, Ferrari M, et al. Oxidative stress and Nrf2 expression in peripheral blood mononuclear cells derived from COPD patients: an observational longitudinal study. *Respir Res*. 2020;21(1):37. doi:10.1186/s12931-020-1292-7
41. Montuschi P. Exhaled breath condensate analysis in patients with COPD. *Clin Chim Acta*. 2005;356(1–2):22–34. doi:10.1016/j.cccn.2005.01.012

42. Agler AH, Kurth T, Gaziano JM, et al. Randomised vitamin E supplementation and risk of chronic lung disease in the Women's Health Study. *Thorax*. 2011;66(4):320–325. doi:10.1136/thx.2010.155028
43. de Batlle J, Barreiro E, Romieu I, et al. Dietary modulation of oxidative stress in chronic obstructive pulmonary disease patients. *Free Radic Res*. 2010;44(11):1296–1303. doi:10.3109/10715762.2010.500667
44. Annesley SJ, Fisher PR. Mitochondria in Health and Disease. *Cells*. 2019;8(7):680. doi:10.3390/cells8070680
45. Bhargava P, Schnellmann RG. Mitochondrial energetics in the kidney. *Nat Rev Nephrol*. 2017;13(10):629–646. doi:10.1038/nrneph.2017.107
46. Giordano L, Gregory AD, Pérez Verdaguer M, et al. Extracellular Release of Mitochondrial DNA: triggered by cigarette smoke and detected in COPD. *Cells*. 2022;11(3):369. doi:10.3390/cells11030369
47. Suski JM, Lebiedzinska M, Bonora M, et al. Relation between mitochondrial membrane potential and ROS formation. *Methods Mol Biol*. 2012;810:183–205.
48. Negre-Salvayre A, Coatrieux C, Ingueneau C, et al. Advanced lipid peroxidation end products in oxidative damage to proteins. Potential role in diseases and therapeutic prospects for the inhibitors. *Br J Pharmacol*. 2008;153(1):6–20. doi:10.1038/sj.bjp.0707395
49. Kirkham PA, Caramori G, Casolari P, et al. Oxidative stress-induced antibodies to carbonyl-modified protein correlate with severity of chronic obstructive pulmonary disease. *Am J Respir Crit Care Med*. 2011;184(7):796–802. doi:10.1164/rccm.201010-1605OC
50. Hu J, Chen C, Ou G, et al. Nrf2 regulates the inflammatory response, including heme oxygenase-1 induction, by mycoplasma pneumoniae lipid-associated membrane proteins in THP-1 cells. *Pathog Dis*. 2017;75(4). doi:10.1093/femspd/ftx044.
51. Xu DD, Chen LL, Chen XS, et al. The triterpenoid CDDO-imidazolide ameliorates mouse liver ischemia-reperfusion injury through activating the Nrf2/HO-1 pathway enhanced autophagy. *Cell Death Dis*. 2017;8(8):e2983. doi:10.1038/cddis.2017.386
52. Wei Y, Lu M, Mei M, et al. Pyridoxine induces glutathione synthesis via PKM2-mediated Nrf2 transactivation and confers neuroprotection. *Nat Commun*. 2020;11(1):941. doi:10.1038/s41467-020-14788-x
53. Motohashi H, Yamamoto M. Nrf2-Keap1 defines a physiologically important stress response mechanism. *Trends Mol Med*. 2004;10(11):549–557. doi:10.1016/j.molmed.2004.09.003
54. Zhang YP, Xi XT, Mei Y, et al. High-glucose induces retinal pigment epithelium mitochondrial pathways of apoptosis and inhibits mitophagy by regulating ROS/PINK1/Parkin signal pathway. *Biomed Pharmacother*. 2019;111:1315–1325. doi:10.1016/j.biopha.2019.01.034
55. Gupta V, Bamezai RN. Human pyruvate kinase M2: a multifunctional protein. *Protein Sci*. 2010;19(11):2031–2044. doi:10.1002/pro.505